Structural studies of Co/Cr multilayered thin films

M. B. Stearns, C. H. Lee, and T. L. Groy*
Department of Physics, Arizona State University, Tempe, Arizona 85287
(Received 20 June 1988)

The structural properties of Co/Cr multilayered structures (ML's) with bilayer thickness varying from 14 to 400 Å and total thickness of about 3000 Å have been studied. These ML's were prepared by *e*-beam vapor deposition of the elemental metals onto temperature-controlled oxidized single-crystal Si substrates. Several sets of multilayers were fabricated in order to investigate various types of effects. It was determined that the multilayer crystallites grow as bcc Cr layers in the [110] direction and hcp Co layers in the [10.1] direction. Crystallites of hcp [00.2] Co and/or [110] Cr and [10.0] Co also occur systematically in some of the ML. The detailed structures of the ML's (the individual layer, bilayer, and interface thicknesses as well as the length of the various crystallites) were determined by modeling the multilayers as having interfaces with a linear variation in composition and fitting the measured large-angle x-ray-scattering spectra to calculated spectra. This analysis indicates that the bilayers of the ML crystallites have asymmetric interfaces as would result from the rate of diffusion or penetration of the Co into Cr being much larger than that of Cr into Co. There is no evidence for any bcc Co. The growth of the ML can be described by three empirical rules. The interface thicknesses of a few ML's having complete alignment were also determined from saturation-magnetization measurements; the two methods gave good agreement.

I. INTRODUCTION

There is strong interest in modifying the properties of materials by alternately depositing two different substances on an atomic level. One of the prime tasks in controlling the properties of such multilayered structures (ML's) is to determine both the chemical and structural order of the films and to try to relate these to the fundamental properties of the two components. The quality of the films, as indicated by the sharpness of interfaces and the degree and type of alignment throughout the ML's, depends on a number of factors, including the bulk crystal structure and atomic sizes or lattice spacings of the two different components, the vacuum or preparation conditions, the rate of deposition, the condition and temperature of the substrate, and, in the case of well-lattice-matched components, on the substrate orientation. Metallic ML's have been classified in several ways depending on the chemical and structural ordering of the two component materials in and between the layers.[1] ML's made from components having a high degree of lattice and structural matching can have single-crystal structure and sharp interfaces, while poorly matched atomic sizes and structures give rise to layers which are strongly compositionally modulated and structurally disordered, or perhaps even amorphous. Thus, in general, the range of the alignment between the layers varies widely depending on the degree of matching between the two components. Large-angle x-ray θ-2θ scattering (LAXS) spectra with the scattering vector perpendicular to the plane of the layers show characteristic interference spectra depending on the *d*-spacing mismatch in the direction of growth. Measurements with the scattering vector in other directions must be made to determine the degree and type of crystalline alignment in these directions.

It should be noted that ML's are usually grown under conditions which are far from equilibrium, and that if quasiequilibrium conditions were used (very slow growth rates with the vapor pressure of the deposit less than the substrate equilibrium pressure) it would be very unlikely to get two-dimensional (2D) crystalline growth since it would require the surface free energies of the two depositing atoms to be equal and the excess interface energy to be negative.[2] Generally, the surface free energies are different, so the laws of thermodynamics would only allow monolayer growth for one of the components. The other component would have island or cluster growth. This has been seen and carefully studied for the fcc Fe-Cu(001) system.[3] The formation of metastable 2D-type layering under nonequilibrium conditions closer to those under which ML's are actually grown has been the subject of many studies and is believed to be dominated by dynamic coalescence.[4]

In this paper we discuss the structural behavior of the Co/Cr ML. We have chosen the Co/Cr system to study since it is of particular interest both for its fundamental magnetic behavior and because it has high potential for application as a medium for perpendicular magnetic recording and information storage. We found that the orientational behavior of Co/Cr ML's as well as other 3*d*-element combinations, where the atomic sizes are similar but the crystal structure is different, can be described by three empirical rules, which are discussed in Sec. III.

Several different series of Co/Cr ML's have been fabricated in order to study various aspects of their behavior. A computer program using a trapezoidal model for the interfaces was previously developed[5] and used to fit the measured (LAXS) spectra of both thin Co films and the ML's. The detailed structural characteristics of the ML's

 ©1989 The American Physical Society

determined using this program are discussed in Sec. IV.

The total interface thickness was also obtained from saturation-magnetization measurements of completely aligned ML's. This is discussed in Sec. IV B.

The magnetic and electronic properties of the ML's are found to strongly depend on the structure of the ML's especially the layer thickness. Thus it is essential to understand the structure of ML's in order to modify controllably the physical properties.

II. SAMPLE PREPARATION

The ML's were prepared by *e*-beam evaporation in an ultrahigh-vacuum (UHV) system. The system consists of two water-cooled, shrouded *e*-beam guns with a reciprocating shutter driven by solenoids. Each gun is monitored and controlled by an Inficon thickness monitor during film growth. A high-speed 8-in. Varian cryopump provides a base pressure of around 5×10^{-10} torr. The growth pressure depends on the evaporation rate, which for the materials used here is about 10^{-8} torr at 1 Å/sec. During the film growth the residual gas pressures were about 5×10^{-9} torr for both N_2 and O_2 and 1×10^{-10} torr for CO_2, so the contamination of these films from residual gases was in the range from 10^{-3} to 10^{-4} monolayers/sec, which is usually negligible. We tried preparing ML's on glass, sapphire, and Si and obtained the best ML's using oxidized single-crystal *p*-type Si(100) substrates of the type commonly used in the semiconductor industry. The surfaces of such substrates are amorphous and smooth to within 2–4 Å. We have confirmed that this is so by examining these substrates in numerous cross-sectional high-resolution transmission-electron-microscopy (HREM) images and find them to be typically flat within an atomic layer over distances of several hundred angstroms. The substrate temperature, measured by a Pt-resistance thermometer embedded in the substrate holder, could be varied between 80 and 700 K. The temperature was controlled by adjusting the flow rate of the liquid nitrogen surrounding the holder or by adjusting the power through a tungsten heating coil embedded in the holder. The deposition temperature was stabilized for about 0.5 h before growing the ML and it was maintained at about ±5 K during the growth. Since Si has a large thermal conductivity the calculated temperature difference between the substrate and the Cu holder was found to be negligible. The Co and Cr targets were 0.5-in. cubes of 99.95% purity. The distance between the centers of the two *e*-beam guns is 5 cm and the distance to the center of substrate is about 20 cm. The area of deposition on the substrate is a square of about 2.5 cm on a side. Thus the angle of incidence and spread of the atomic beams is $8°\pm3°$ from the normal, and neglecting the source size a given layer thus has a maximum variation in thickness of about 5% from geometric effects.

The bilayer thicknesses Λ were determined in four ways. The first was by measuring the total thickness using a Dektak surface profiler and dividing by the number of bilayers determined by a counter which recorded the shutter movement. This is the least accurate measurement since the accuracy of the total thickness measurements seems to be no better than $\sim10\%$. The second method obtained Λ from the computer modeling of the large-angle x-ray spectra. The third was to obtain Λ from the corrected small-angle x-ray scattering (SAXS). The fourth obtained Λ from the spacing of the spots due to the layering in electron diffraction patterns of cross-sectional samples of the ML's. The four methods gave good agreement.

III. EPITAXIAL GROWTH BEHAVIOR OF ML'S

In general the growth of thin films involves adsorption, nucleation, clustering, surface diffusion, evaporation, coalescence, chemical binding, and other atomic processes at the surface.[4,6] The growth direction thus depends on a number of factors having small energy differences. Since the 3*d* metals have high coercive energies, they would tend to have 3D (Volmer-Weber) cluster growth when grown near thermodynamic equilibrium conditions. However, metallic ML's are usually grown under such high supersaturation conditions that the large driving force, $\Delta\mu$ causes kinetic growth to dominate. This can allow metastable 2D growth to occur due to the rapid diffusion of the adatoms. Under conditions where good alignment in the growth direction is obtained, e.g., for the Co/Cr ML at deposition rates of ~1 Å/sec and substrate temperature around room temperature, the supersaturation ratio P/P_s is about 10^{48}, so the driving force $\Delta\mu=kT_s\ln(P/P_s)=110kT_s$. Thus when the deposition is carried out very far from equilibrium conditions the domination of kinetic growth apparently allows 2D-like growth to occur. Moreover, in our case, the substrate is oxidized Si having an amorphous surface, so the substrate does not play a role in determining the growth orientation.

In spite of the growth of these ML's being mainly determined by kinetics, it appears that the growth orientation of each of the layers is mainly determined by the surface free energy of the various crystallographic faces of the two deposited components. Under these conditions we find that the growth of these ML's can be described by three empirical rules.

Rule 1. The first rule results from the well-known ordering of the preferred crystallographic growth directions obtained from free-surface-energy calculations for flat smooth surfaces considering only pairwise bonding.[7] An overly simplistic view (but one that often gives the correct order of preferred orientations) is that a negative energy results from each bond and therefore the surface energy is smaller the greater the number of bonds between atoms in the given surface plane. Thus, roughly speaking, the favored crystal orientations are those having the smallest area per atom in the film plane (largest in-plane density) or, equivalently, the direction which has the largest *d* spacing between planes. This is generally the case for bcc and fcc components of ML's. At high substrate temperatures other considerations and growth mechanisms can become important and cause other orientations to dominate.[4]

Rule 2. The second empirical rule has the same type of origin as the first when applied to growth across interfaces of chemically similar materials. It is that for small layer thicknesses the dominant growth direction is that which minimizes the energy by maximizing the number of bonds across the interfaces. This is achieved by choosing the direction of growth across the interface which keeps the area per atom for the two ML components as nearly equivalent as possible. This rule is very different from those which apply to a perfect-crystal-type ML where the azimuthal orientation is dictated by the geometry of the various structures and the substrate. For the Co/Cr ML there is minimal azimuthal registry across the layers. For ML systems where the area per atom of the two components is very different, this rule appears to become that growth is favored when the ratios of the area per atom vary as $(n+1)/n$, where n is a small integer. Here there is often a geometric epitaxy as the atoms of the two components go into a high degree of registry. An example of such a system is the Au/Co ML,[8,9] where $n=3$ and the atoms in the (111) planes of Au are in excellent registry with the atoms in the plane of (00.2) Co when these planes align so that the [220] direction of Au is along the [11.0] direction of Co.

Rule 3. The third empirical rule is that if there is a tendency for alignment in the direction of growth across the interfaces in the ML the element which controls the overall orientations is that which has the greatest difference in surface free energy, i.e., the largest difference in area between the closest-packed orientations. Below we discuss how these rules are seen to apply in the Co/Cr ML. We have also found them to apply for several other ML systems, e.g., Ni-Cr, Ni-Mn, and Co-Mn.[10]

In Table I we list the area per atom in Å^2 for the crystallographic planes having the highest in-plane densities for bcc Cr and various types of Co. In agreement with rule 1 we find that, on the nonlattice-matched oxidized Si substrates, Cr grows with the [110] direction normal to the substrate. However, the more complex structure of the hcp lattice has three directions, [10.0], [00.2], and [10.1], which have similar area per atom. It is found that thin films of pure Co grow in all three of these directions, so, within this limitation, rule 1 also applies to Co. Since the area per atom is similar for the three directions, other considerations become important in determining the distribution between them in thin Co films.

TABLE I. The d spacings, in area per atom, and Bragg-peak positions for Cr $K\alpha$ for the crystal orientations having the smallest area per atom.

Orientation	d spacing (Å)	Area per atom (Å^2)	2θ (deg)
hcp [10.0] Co	2.150	5.12	64.3
hcp [00.2] Co	2.031	5.48	68.6
hcp [10.1] Co	1.916	5.80	73.4
bcc [110] Cr	2.039	5.88	68.3
bcc [110] Co[a]	1.9891	5.60	70.3
fcc [111] Co	2.046	5.44	68.05

[a]Calculated assuming constant volume per atom for the bcc and hcp crystal structures.

IV. SAMPLE CHARACTERIZATION

A. From x-ray spectra

The x-ray spectra were measured with a Rigaku RU200B rotating-anode diffractometer using Cr K_α radiation. Thus the longitudinal coherence of the x-ray beam is about 1 μm. The instrumental resolution was 0.15°, so the lateral coherence is about 1000 Å.

1. Computer model used to analyze LAXS

The shape of the x-ray spectra of ML's, including various models for the interfaces, has been calculated by several groups.[1,11,12] We have extended these calculations by developing a computer program having interfaces with a linear composition profile and pure crystallites with two types of orientation. The details of this program have been presented previously.[5] A schematic diagram of the assumed d-spacing variation with layer number is given in Fig. 1. The d spacings, atomic-scattering factors, Debye-Waller factors, and in-plane densities of the atoms are all assumed to vary linearly across an interface. This is the type of variation which would result from a completely miscible alloy system, and although Co and Cr have limited miscibility under equilibrium conditions it is assumed that they are essentially miscible for the highly nonequilibrium conditions under which these ML's were grown. This intermixing at the interfaces of ML's has been clearly seen in many HREM images of several systems which we have published elsewhere.[10,13,14] The assumed linear variation of properties

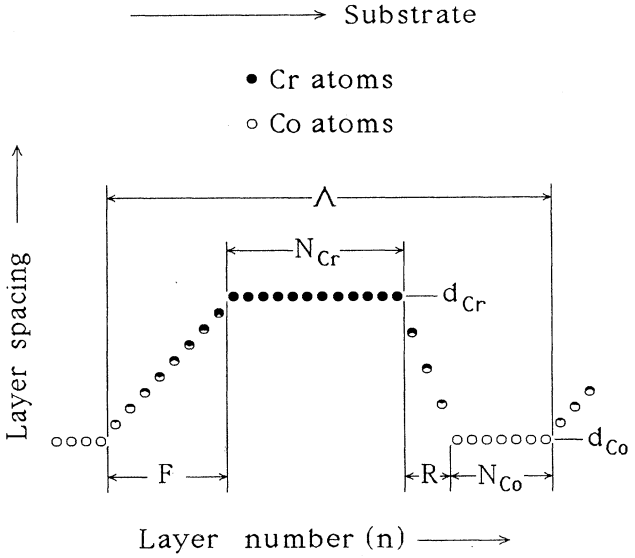

FIG. 1. Schematic diagram of the variation of the d spacing with the layer number for the linear-interface model. The layer numbers are sequenced as seen by an incoming x ray, not as grown from the substrate.

across the interface is not to be taken too literally, but as a first approximation to the actual functional form of the variation. We realize that a composition distribution which merges smoothly into the pure regions is much more likely. Such deviations from a linear variation would mainly have a small affect on the magnitudes of the higher-order satellites. Thus in this analysis we concentrate on fitting the first- (and sometimes the second-) order satellites. For all the spectra we analyzed, the number of features in the measured spectra (see Ref. 5) is equal to or greater than the number of parameters determined from the fit, so these parameters are uniquely determined.

It was found that the spectra could be fitted excellently with a model having three types of crystallites: (1) multilayer crystallites (MLC's) made up of layers having hcp [10.1] Co and [110] Cr orientations, (2) pure [00.2] Co and/or [110] Cr (denoted as B type; since these have very similar d spacings, they are not separable in the spectra), and (3) pure [10.0] Co (denoted as C type). At high substrate temperatures (>400 K) some of the crystallites of Co may also be in the fcc [111] orientation, which has a d spacing very close to that of hcp [00.2] Co. Typical spectra of the Co/Cr ML are shown in Figs. 2 and 3. As can be seen for individual layer thicknesses of less than about 35 Å, this system shows the well-known type of interference spectrum consisting of a central peak flanked by satellite peaks. The well-defined structure of these ML's is ideal for this type of analysis due to the d spacings of the two main orientations differing by about 6%. It was found that many of the structural parameters characterizing the ML's are essentially independent of one another. These parameters and their sensitivity to particular features of the spectra are now listed.

(1) The position of the central peak is sensitive to the relative number of Cr, N_{Cr}, and Co, N_{Co}, atomic layers in the pure regions of the layers, see Fig. 1.

(2) The heights of the satellites relative to the main peak are sensitive to the number of interfacial layers F and R.

(3) The angular difference between the first upper and lower satellites depends on the bilayer thickness, $\Lambda=(F+R)\bar{d}+N_{\mathrm{Cr}}d_{\mathrm{Cr}}+N_{\mathrm{Co}}d_{\mathrm{Co}}$, where d_{Cr} and d_{Co} are the d spacings of [110] Cr and [10.1] Co, and $\bar{d}=(d_{\mathrm{Cr}}+d_{\mathrm{Co}})/2$.

(4) The widths of the peaks are determined by the lengths of the crystallites, i.e., the number of atomic layers, in the direction of growth. Let L_M, L_B, and L_C denote the average lengths of the MLC's, B-type crystallites and [10.0] Co crystallites, respectively. L_M is obtained from the number of bilayers needed to fit the width of the ML peaks plus a fractional correction factor for additional broadening due to a noninteger number of bilayers.[5]

Since, in general, we do not know the in-plane area of the crystallites, only the area fractions of each crystallite type can be uniquely determined in fitting the spectra. These are defined as follows: Let n_B and n_C be, respectively, the ratios of the number of type-B and -C crystallites to the number of MLC's in a unit volume, and A_B and A_C the ratios of the average in-plane areas of type-B and -C crystallites to the average in-plane area of the average MLC. Then the linear fractions of crystallites B and C are given by

$$f_B=n_B A_B^2,\quad f_C=n_C A_C^2\ , \tag{1}$$

respectively. The area fraction of the MLC's is $1-f_B-f_C$. At present we have not yet determined A_B and A_C, so we cannot determine the volume fraction of each crystallite type. These quantities can be obtained from x-ray scattering with the wave vector near the plane of the ML, and these experiments are planned. Since the crystallites are not well aligned in the plane of the films, these scattering intensities are expected to be small, and these measurements will probably need to be done using synchrotron radiation. In the meantime there are two cases of crystallite shapes for which the volume fractions can be easily evaluated. These cases are the following.[5]

Case (a). All the crystallites have the same in-plane areas, i.e., $A_B=A_C=1$. In this case the volume fractions are given by

$$v_{\mathrm{ML}}=1/g,\quad v_B=f_B L_B/gL_M\quad v_C=f_C L_C/gL_M\ , \tag{2}$$

where $g=1+f_B L_B/L_M+f_C L_C/L_M$.

Case (b). Each type of crystallite is the same size in all directions. We found that this case does not seem to correspond to the growth of the ML. Because of the small scattering power of small crystallites, this case gives unreasonably large volume fractions for the smaller crystallites. Because of this the results of this type of assumption will not be presented and all the volume fractions quoted are for the assumption of equal in-plane areas.

2. *Thin films of Co*

A θ-2θ x-ray-diffraction spectrum for a pure Co film of $\sim$3000–5000 Å thickness deposited on an oxidized Si substrate at room temperature is composed of three peaks corresponding to the three preferred directions [10.0], [00.2], and [10.1]. These spectra look quite similar to the ($\sim$200 Å)/(200 Å) spectrum in Fig. 3. The results of the analysis of the spectra from three different Co films with our computer program are listed in Table II. It is seen that the crystallite lengths for the [10.0] and [00.2] directions of growth are similar at $\sim$150–200 and $\sim$180–200 Å, respectively, while those for the [10.1] crystallites are $\sim$40 Å. The d spacings for Co films deposited at a substrate temperature of 500 K approach the bulk values more closely than these films and the crystallite lengths for the [10.0], [00.2], and [10.1] directions are 150, 400, and 33 Å, respectively. This type of behavior is expected due to the different multiplicity factors (6, 2, and 12, respectively) for the three directions plus the highly irregular atomic distribution of the atoms in the (10.1) planes.

In Table II we also list the measured d spacings for bulk and powder samples[15] of Co. It can be seen that the crystallites growing in the [10.0] direction are contracted in that direction relative to this d spacing in a powder or in the bulk. Crystallites growing in the [00.2] direction are expanded in that direction compared to those of a

powder and contracted compared to the bulk d spacing, while those oriented in the [10.1] direction are slightly expanded relative to a powder or bulk sample. Since the volume per atom is expected to remain nearly the same in all the crystallites the c axis is probably expanded in [10.0] crystallites, while the average spacing in the (10.1) plane is contracted in the [10.1] crystallites. Thus for room-temperature substrates the [10.0] and [10.1] crystal-

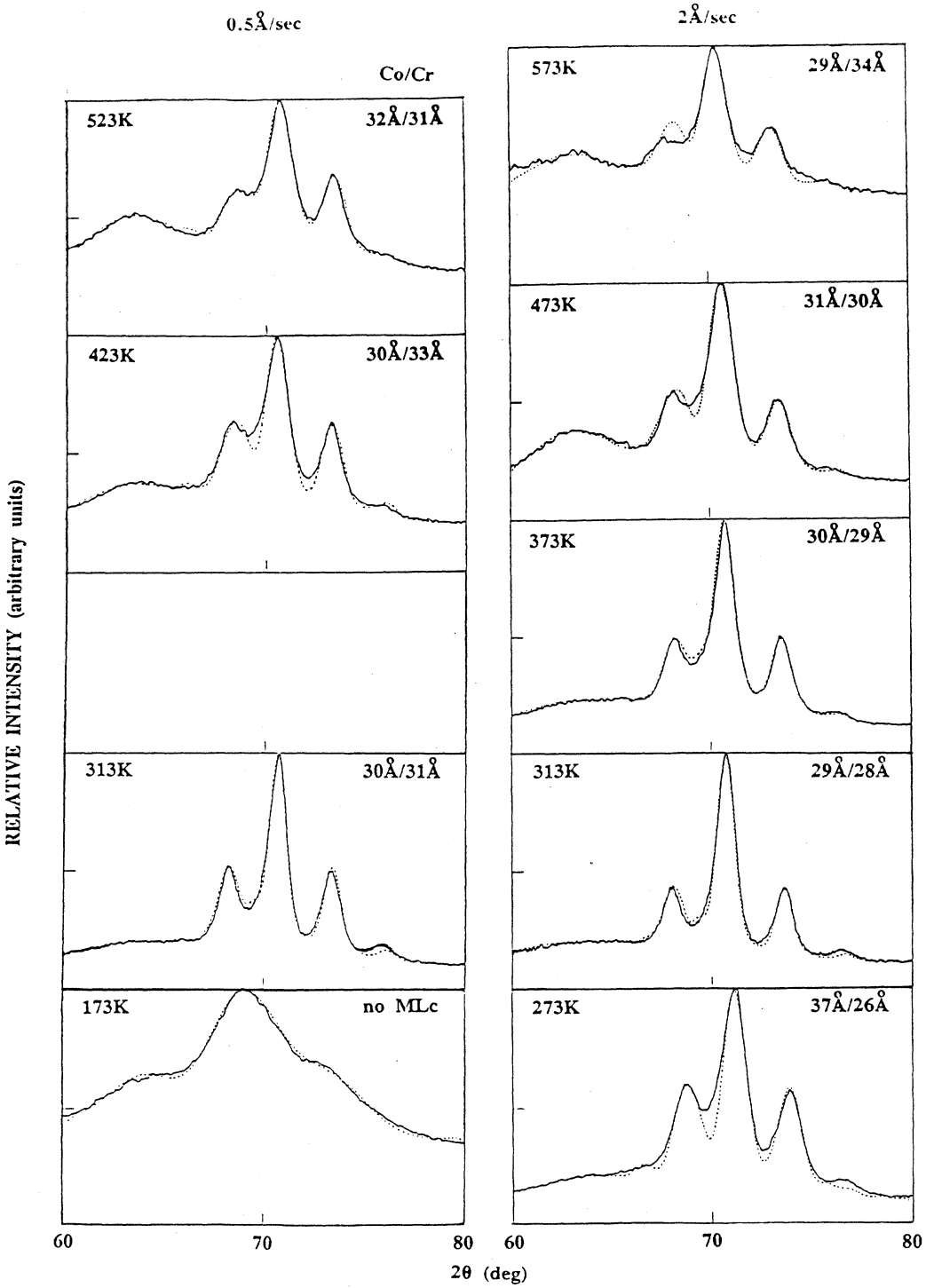

FIG. 2. Measured and calculated Cr $K\alpha$ θ-2θ x-ray spectra of a series of nominally 30 Å Co/30 Å Cr ML's fabricated at various substrate temperatures and deposition rates of 0.5 and 2 Å/sec. The solid and dotted curves are the measured and calculated spectra, respectively.

lites of pure Co films grow with considerable strains built into them.

The area fractions and the volume fractions assuming equal in-plane cross-sectional areas for all the crystallites are also listed in Table II. It is seen that under this assumption the volume fraction of the [10.0] crystallites is about 10%, while those of [00.2] and [10.1] are comparable. However, there is no evidence at present that the in-

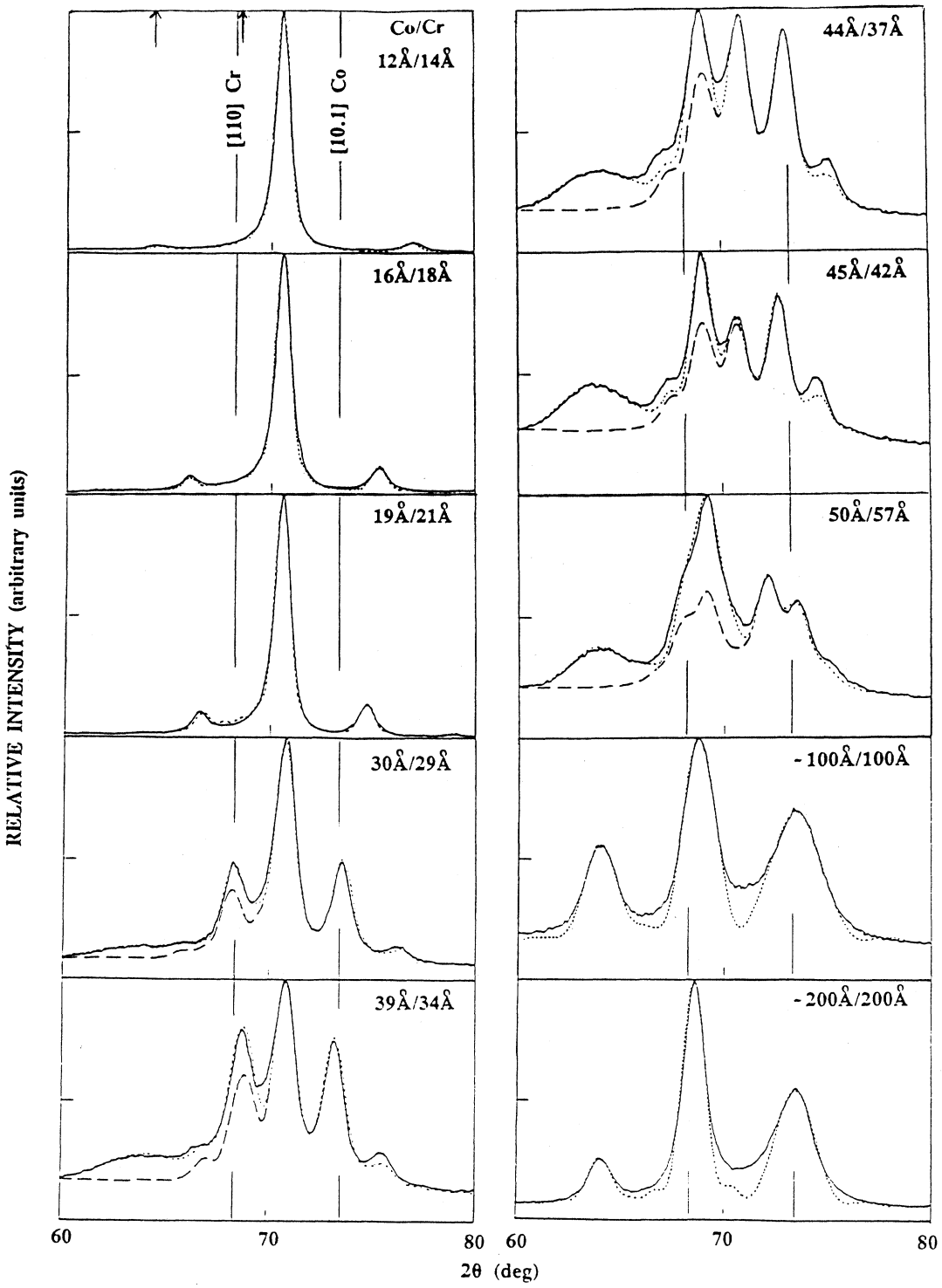

FIG. 3. Measured and calculated Cr $K\alpha$ θ-2θ x-ray spectra of a nominally equal-layer-thickness series of Co/Cr ML's. The solid and dotted curves are the measured and calculated spectra, respectively. The dashed curve corresponds to the spectra due to the MLC's only, without any crystallites of pure Co and Cr. The vertical lines indicate the positions of the scattering peaks for pure [110] bcc Cr and [10.1] hcp Co. The arrows show the positions for hcp [10.0] and [00.2] Co.

TABLE II. Crystallite sizes in the direction of growth and d spacings and fractions of pure Co films deposited at room temperature on an oxidized Si substrate. The orientations are denoted by $a=[10.0]$, $b=[00.2]$, and $c=[10.1]$.

Nominal thickness (Å)	Lengths (Å)			d spacing (Å)			Area fractions	Volume fractions (%)
	a	b	c	a	b	c	f_b,f_c	a,b,c
5000 [(2 Å)/s]	172	192	40	2.150	2.027	1.914	0.32,0.07	11,54,35
3000 [(1 Å)/s]	152	203	40	2.145	2.031	1.918	0.40,0.08	9,61,30
3000 [(1 Å)/s]	205	183	43	2.155	2.035	1.916	0.19,0.04	10,43,47
Average d spacings				2.150	2.031	1.916		
Powder				2.165	2.023	1.910		
Bulk				2.171	2.035	1.912		

plane areas of the different-type crystallites are the same; we only use this type of assumption to obtain a rough estimate of the volume fractions. The area fractions for Co films were found to be quite independent of the substrate temperature. More details of dependence of the structure of pure Co films on the substrate temperature and deposition rate will be published elsewhere.

3. *Co/Cr ML*

According to rule 2, for small layer thicknesses, the growth direction will be that in which the area per atom for the two components are the closest. As seen in Table I, [10.1] hcp Co has the closest area per atom to that of [110] Cr; the difference is 1.4%. We have found that indeed all the Co/Cr MLC's grow with the Co oriented only in the [10.1] direction. The ML films with layer thicknesses of >20 Å of Co also have pure Co and Cr crystallites, but the [10.0] and [00.2] Co orientations are not present in the MLC's. The origin of the pure crystallites is believed to be due to the well-known columnar growth in CoCr alloys.[16] This columnar structure is also seen in HREM images of these Co/Cr ML's.[10,14]

(a) *Dependence of the growth parameters on the substrate temperature and deposition rates.* At present few systematic studies of the dependence of the properties of ML's on the deposition parameters have been reported.[17,18] In order to study the effects due to different deposition parameters, we have fabricated a set of nominally (30 Å Co)/(30 Å Cr) ML's over a substrate temperature range from 170 to 530 K at the two deposition rates of 0.5 and 2 Å/sec. The large-angle Cr $K\alpha$ θ-2θ x-ray spectra for these ML's are shown in Fig. 2. The solid lines are the measured spectra, while the dotted lines show the spectra calculated with the linear interface model for symmetrical front and rear interfaces. The parameters obtained from the fitted spectra are listed in Table III. The films grown at 173 K showed no evidence of forming multilayers. Their spectra could best be fitted with small crystallites of pure Co and Cr. The crystallite sizes in the direction of growth are listed in Table III. As can be seen, the background for this film is large, indicating a large fraction of unaligned grains. The films grown at 273 K and above all have MLC's as well as crystallites of pure Co and Cr. For $T_s>420$ K the fraction of aligned crystallites decreases with increasing T_s, as indicated by the increase in the background with increasing T_s. The maximum intensity of the scattered x rays did not vary appreciably over the whole temperature range. This is in contrast to earlier reported results,[19] but the measure-

TABLE III. Variation of derived parameters of nominally (30 Å Co)/(30 Å Cr) multilayers fabricated at different substrate temperatures T_s and deposition rates. The different types of crystallites are denoted MLC, or multilayer; $B=[00.2]$ Co and/or [110] Cr, and $C=[10.0]$ Co. L_M, L_B, and L_C are their lengths in the direction of growth. F and R are the front and rear interfaces as shown in Fig. 1.

Co/Cr (Å)	T_s (K)	F,Cr,R,Co (no. of layers)	Λ (Å)	L_M (Å)	L_B,L_C (Å)	f_B,f_C	v_{ML},v_B,v_C (%)	Background (%)
				Deposition rate of 2 Å/sec				
37/26	273	8,5,8,11	63	113	91,22	0.12,0.85	80,7,13	11
31/26	313	8,5,8,8	57	141	61,26	0.22,1.0	79,7,14	12
29/28	313	9,5,9,6	57	155	61,17	0.18,2.2	76,5,19	12
30/29	373	8,6,9,7	59	139	61,19	0.22,1.7	75,7,18	13
31/30	473	10,5,10,6	61	103	72,28	0.11,1.1	73,6,21	15
29/34	573	9,8,9,6	63	106	72,26	0.10,1.5	69,5,26	38
				Deposition rate of 0.5 Å/sec				
	173	no MLC's		[10.1]=27 Å, B=41 Å, C=17 Å			35,30,35	37
30/31	313	8,7,9,7	61	157	61,22	0.28,1.2	79,8,13	12
30/33	423	8,8,9,7	63	113	101,22	0.06,1.4	76,4,20	21
32/31	523	7,8,8,9	63	102	100,26	0.04,1.3	73,3,24	28

ments reported here were taken much more carefully and with better statistics.

As seen from Table III, the coherence length L_M of the MLC's is largest, ~ 160 Å, near $T_s \sim 310$ K. It then decreases and levels off for substrate temperatures ≥ 420 K. The lengths in the growth direction are $\sim 60-100$ Å for the type-*B* crystallites and ~ 25 Å for the [10.0] Co crystallites. There may also be a small amount of fcc [111] Co present, but it cannot be identified in the x-ray spectra. A small amount is believed to have been seen in the electron diffraction and HREM images. As seen in Table III, the interfaces of this series are about eight to nine atomic-layers thick for a symmetric profile [or a total interface thickness of about 12 atomic layers for a completely asymmetric profile, see subsection (b)] and are quite independent of T_s. The saturation-magnetization values, M_s, of this ML series were essentially constant, also in agreement with there being no appreciable change in the interface thickness over this temperature range.

Assuming equal in-plane areas, the volume fraction of the MLC's is predominant and decreases slightly with increasing T_s; that of the type-*B* crystallites is about 6%, while that of the [10.0] Co crystallites increases with increasing T_s from $\sim 13\%$ near 270 K to $\sim 25\%$ near 550 K.

Since the best ML films, as judged by the degree of alignment and the length of the MLC's, are those made at $T_s \sim 310$ K, the subsequent series of ML's were made using this substrate temperature and a deposition rate of 1 Å/sec.

(b) *Equal-layer-thickness ML's.* In order to investigate the behavior of the growth of Co/Cr multilayers, we fabricated a series of ML's with nominally equal Co and Cr layers over layer thicknesses from 7 to 200 Å. The θ-2θ spectra of some of these ML's are shown in Fig. 3. The usual evolution of the interference spectra typical of ML's is clearly seen.[20] The spectra were analyzed with two extreme types of composition profiles: a symmetric one where the front and rear interfaces were assumed to be of equal thickness (model *S*), and a completely asymmetrical one where all of the interfacial thickness is in one of the interfaces (model *A*). From the analysis of these ML's we found that both the symmetric and a particular type of antisymmetric interface model gave equally good fits to the spectra of this series. The *A* profile that fit well was that of the front interface, *F*, having all the interfacial width followed by the pure Cr region and then a sharp drop to the pure Co region, i.e., $R = 0$. Letting *T* represent the thick interface in model *A*, the bilayer order is *T*/Cr/0/Co (the substrate is on the right side of this sequence, see Fig. 1.). The interchanged interface order 0/Cr/*T*/Co never gave good fits. This asymmetric-type profile would result if the Co diffused or penetrated into the Cr as it was deposited, while the Cr did not go into the Co. The results of fitting to models *S* and *A* (symmetric and asymmetric, respectively) are tabulated in Table IV. In general, the amount of interface for the completely asymmetrical interfaces is approximately four layers less than for the *S* model because the asymmetric interfaces give rise to slightly smaller satellites as compared to the main interference peak. It is seen that the parameters for the two different profiles are nearly the same except for slightly larger pure regions for the asymmetric interfaces. It was found that the 21-Å Co series was very sensitive to the symmetry of the interfaces as discussed in the next section; for this series model *A* was definitely preferred.

Another question that could be examined was whether the MLC's tended to terminate in a particular order. If the growth terminated near the start of a Co layer, the order of the bilayers would be *T*/Cr/0/Co, whereas if it terminated near the end of a Co layer it would be 0/Co/*T*/Cr. We found that the termination effects were negligible when the MLC's consisted of four or more bilayers. However, for MLC's having three or fewer bilayers only the particular bilayer order *T*,Cr,0,Co gave good fits; 0,Co,*T*,Cr did not. The poor-fitting spectra had characteristic peak spacings that were very different from the measured spectra. This indicates that the MLC's tend to grow in a definite configuration.

For layer thicknesses of ≤ 20 Å the films were predominantly composed of oriented MLC's containing only [10.1] hcp Co and [110] bcc Cr. Thus rule 2 was found to determine the ML growth. We also tried other combinations of ML growth, such as [10.1] Co followed by [00.2] Co, but all other combinations gave very poor fits to the data. It should be noted that rule 2 applies for the [10.1] Co direction in spite of the irregular position of the atoms in this orientation. Here the Co atoms do not lie in well-defined (10.1) planes but are considerably dispersed in the [10.1] direction with their projection on the (10.1) plane being quite jumbled. The distribution of atoms in this direction is more like an amorphous structure than a smooth crystalline plane.[10]

It can be seen from Table IV and Fig. 4 that the ~ 7-Å-layer-thickness MLC's is essentially all interface and that it grows coherently for about nine bilayers. The MLC lengths in the direction of growth are largest for $\Lambda = 25-35$ Å, where they are comprised of six to eight bilayers. Then, as the layer thickness increases L_M decreases in length. However, whereas L_M has a maximum, the number of coherent bilayers decreases with layer thickness continuously over the whole series. At $\Lambda \geq 26$ Å oriented crystallites of pure Co and Cr appear and increase in volume and length. For $\Lambda \sim 80$ Å and above L_M stays constant at ~ 130 Å. This, plus the fact that in the 21-Å Co series, as discussed below, the MLC's having thicker Cr layers are coherent over longer distances, indicates that the weaker link in maintaining the MLC coherence is the [10.1] Co layer. This is not unexpected since, as seen in Table II, even in pure Co films the average size of crystallites growing in the [10.1] direction is only about 40 Å. As seen from Table IV, the length and area fraction of type-*B* and [10.0] Co crystallites increase with layer thickness. The *B* crystallites increase from 50 to 130 Å, while the [10.0] Co crystallites are smaller and vary from 20 to 40 Å. Assuming equal in-plane areas, the volume fraction of MLC's decreases continually with increasing Λ down to $\sim 60\%$ for $\Lambda \sim 100$ Å. As seen from the increasing background, the amount of unaligned crystallites also increases with layer thickness.

In Fig. 5 we show the variation of the number of inter-

TABLE IV. Derived parameters for the nominally equal-layer-thickness series. The multilayers marked with an asterisk were deposited at 2 Å/sec; all others were at 1 Å/sec. S and A denote symmetric or asymmetric profiles. F and B are the front and rear surfaces.

Co/Cr (Å)	F,Cr,R,Co (no. of layers)	Λ (Å)	L_M (Å)	L_B,L_C (Å)	f_B,f_C	v_{ML},v_B,v_C (%)	Background (%)
6/8S*	3,1,3,0	14	125	0,0	0,0	100,0,0	1.5
6/8A*	4,2,0,1	14	125	0,0	0,0	100,0,0	
12/14S*	6,1,7,0	26	194	51,0	0.05,0	99,0,0	1.5
12/14A*	10,2,0,1	26	194	51,0	0.05,0	99,0,0	
16/19S	6,3,7,2	35	195	50,0	0.10,0	98,2,0	2
16/18A	10,4,0,3	34	190	40,0	0.12,0	98,2,0	
19/21S	7,3,7,3	40	187	51,0	0.06,0	98,2,0	1.5
19/21A	11,5,0,4	40	187	51,0	0.10,0	97,3,0	
23/20S*	8,2,8,4	43	157	51,0	0.18,0	94,6,0	1
22/19A*	11,4,0,6	41	150	51,0	0.24,0	92,8,0	
28/29S*	9,5,10,5	57	155	102,0	0.11,0	93,7,0	3
28/29A*	15,7,0,7	57	155	102,0	0.11,0	93,7,0	
28/29S	8,6,9,6	57	147	102,24	0.80,0.50	92,5,3	8
27/30A	12,9,0,8	57	147	102,24	0.08,0.40	89,5,6	
30/29S	7,7,8,8	59	146	102,26	0.10,0.55	91,6,3	8
30/29A	11,9,0,10	59	146	122,26	0.08,0.40	89,5,6	
34/31S*	10,5,11,7	65	147	102,28	0.22,0.20	85,12,3	7
34/31A*	15,8,0,10	65	143	102,28	0.20,0.20	85,12,3	
39/34S	10,7,10,10	73	128	122,30	0.09,0.48	84,7,9	14
41/34A	16,9,0,13	75	126	122,30	0.11,0.48	82,9,9	
44/37S	11,7,11,12	81	129	122,37	0.10,0.48	81,8,11	15
48/35A	17,9,0,16	83	132	122,37	0.14,0.50	79,10,11	
45/42S	11,10,11,12	87	137	131,39	0.14,0.78	74,10,16	22
45/42A	14,14,0,16	87	137	131,39	0.12,0.72	75,9,16	
48/51S[a]	9,16,9,16	99	127	131,34	0.22,0.35	76,17,7	10
48/51A[a]	14,18,0,18	99	127	131,34	0.20,0.32	77,16,7	
50/57S[a]	10,18,10,16	107	132	70,43	0.85,0.66	62,26,12	16
50/57A[a]	16,20,0,18	107	132	70,43	0.85,0.66	62,26,12	
~(100 Å)/(100 Å)	no MLC's [10.1]=57 Å, B=91 Å, C=71 Å				0.53,0.11	33,43,24	8
~(200 Å)/(200 Å)	no MLC's [10.1]=69 Å, B=122 Å, C=110 Å				0.58,0.12	45,46,9	6

[a]The parameters of these ML's, which had no central peak and appreciable B crystallites, were quite interactive, so they are not as well determined as for the other ML's.

face layers with Λ as obtained by using models S and A. It is seen that for $\Lambda < \sim 70$ Å the interface thickness increases with increasing Λ; above 70 Å it remains constant. This leveling off of the interface thickness is not a general property of ML's. We have seen other systems where this does not occur and the interfaces just continue to get thicker with layer thickness, e.g., the V/Cr ML system. The A model is seen to give total interface thicknesses which are two to six layers less than that of the S model.

In another study on the Co/Cr ML the main interference peak was incorrectly identified as being due to bcc Co.[21] As seen from Table II, the area per atom for [110] bcc Co is not nearly as well matched to [110] Cr as that of [10.1] hcp Co, so it is not favorable to form bcc Co in these ML's. Electron diffraction photographs also give no indication of any bcc Co in these ML.[10,14]

(c) *21-Å Co series.* A series of ML's having a fixed nominal value of 21 Å of Co and Cr layer thicknesses varying from 14 to 60 Å was fabricated in order to investigate the dependence of the magnetization on the intervening Cr layer thicknesses. While the magnetization did decrease systematically, as will be presented elsewhere, it is necessary that the structure be well characterized in or-

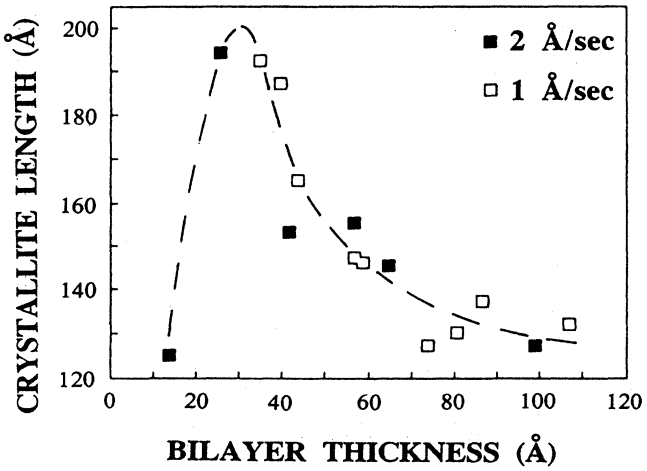

FIG. 4. Variation of the length in the direction of growth with bilayer thickness Λ for the ML crystallites of the nominally equal-layer-thickness series.

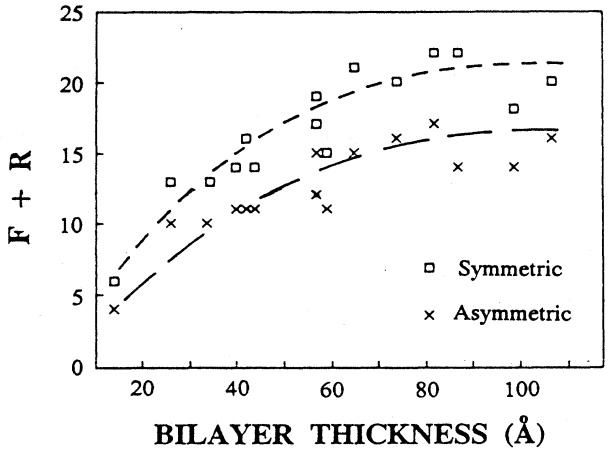

FIG. 5. Variation of the total interface thickness, in number of layers, with Λ for the MLC's of the nominally equal-layer-thickness series.

der to be able to interpret the magnetization measurements correctly.

The parameters obtained by fitting the measured spectra to the linear-interface computer models are listed in Table V. The measured and calculated spectra are shown in Fig. 6. As can be seen, this series had some striking features. One is, in contrast with the behavior of the nearly-equal-thickness series, that the linewidths decrease with increasing Cr content. This can be clearly seen from the essentially linear increase of L_M from ~160 Å at $\Lambda=35$ Å to ~210 Å at $\Lambda=86$ Å. This again indicates that it is the [10.1] Co layers that are responsible for the loss in coherence of the MLC's. The pure type-*B* crystallites are seen to increase in length from 40 to 160 Å as Λ increases. Another noticeable feature (which was also true, but not as obvious, for the equal-layer-thickness series) is that the widths of the satellites are essentially the same as that of the central peak. For $\Lambda > 70$ Å the interfaces of this series are thicker than for the equal-layer-thickness series with essentially all of the Co going into the interfaces.

From the analysis of the equal-layer-thickness ML's, we saw that both the symmetric and antisymmetric interface models gave essentially equally good fits to the spectra. However, for this series the interface distribution which gave the best fit to each spectrum is indicated by superscript b in Table V. Thus we found that this series showed behavior similar to the equal-thickness ML's, the difference being that for all the ML's having Cr layers thicker than 21 Å better fits were obtained with the

TABLE V. Derived parameters for the nominal 21-Å Co series. *F* and *R* are the front and rear surfaces.

Co/Cr (Å)	*F*,Cr,*R*,Co (no. of layers)	Λ (Å)	L_M (Å)	L_B,L_C	f_B,f_C	V_{ML},V_B,V_C (%)	Background (%)
21/14*S*	6/1/6/5	35	159	40[a],33	0.35,0.15	89,8,3	2
21/14*A*	8/3/0/7	35	159	40[a],33	0.35,0.15	89,8,3	
22/22*S*	7/4/7/4	44	165	51[a],0	0.25,0	93,7,0	2
22/22*A*	11/6/0/5	44	165	51[a],0	0.10,0	97,3,0	
21/29*S*	9/5/10/1	50	187	124,0	0.06,0	96,4,0	6
20/30*A*[b]	14/8/0/3	50	192	124,0	0.12,0	93,7,0	
26/42*S*	13/8/13/0	68	191	164,0	0.11,0	91,9,0	13
25/43*A*[b]	23/10/0/1	68	191	164,0	0.19,0	86,14,0	
26/50*S*	13/12/13/0	76	207	164,0	0.13,0	91,9,0	10
26/50*A*[b]	26/12/0/0	76	213	164,0	0.33,0	80,20,0	
29/57*S*	13/16/12/2	86	208	163,43	0.19,0.4	81,12,7	12
29/57*A*[b]	25/16/0/2	86	208	163,43	0.42,0.4	71,23,6	

[a]*B* crystallites were assumed to be for [00.2] Co; for all ML's with $\Lambda \geq 50$ Å they were assumed to be [110] Cr.
[b]These parameters gave a better fit.

asymmetric model where all interface thickness was in front of the pure-Cr region. The analysis does not have the sensitivity to accurately determine the degree of the asymmetry, but definitely indicates that the Co atoms penetrate into the Cr layers to a greater degree than do the Cr atoms into the Co layers. Other profiles with a maximum Co content of less than 100% were tried, but these spectra gave even poorer fits than those obtained for symmetrical interfaces.

The observed behavior is consistent with recent diffusion data[22] which showed that the mobility of an atomic species in a given lattice strongly depends on the atomic size. There it was found that the diffusion coefficient of Co in amorphous $Ni_{50}Zr_{50}$ was $\sim 10^3$ greater than that of the larger Cr atom although the atomic radius of Cr is only $\sim 3\%$ larger than that of Co. Furthermore, the hcp Co lattice is a more densely packed lattice than that of bcc Cr, so it may well be that the Co diffuses or penetrates considerably more rapidly into the Cr layers than vice versa.

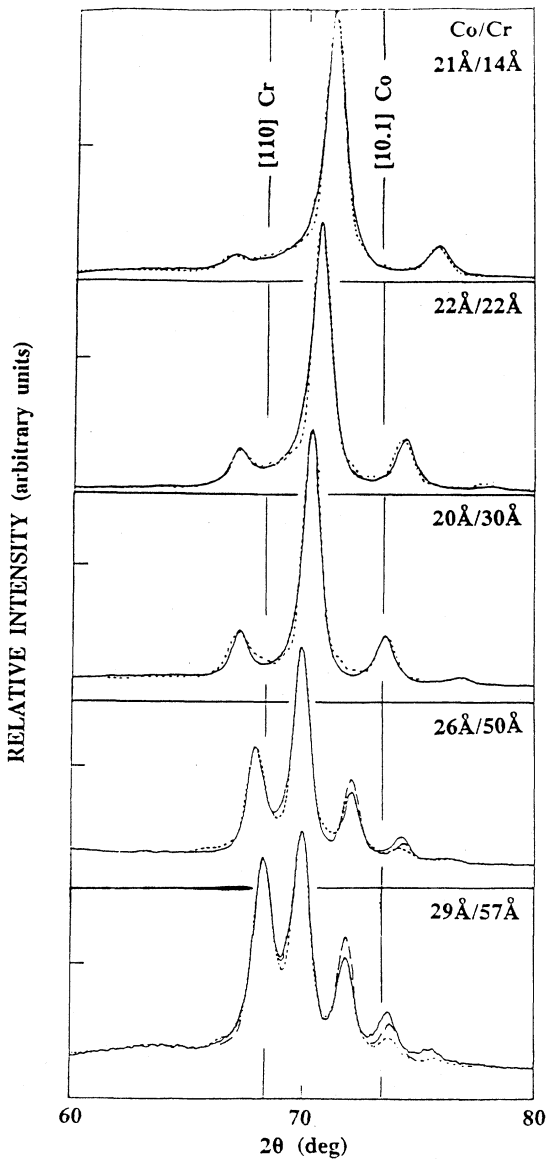

FIG. 6. Measured and calculated Cr $K\alpha$ x-ray spectra for the nominal 21-Å Co series. The solid and dotted curves are the measured spectra and the calculated spectra for asymmetric interfaces, respectively. The dashed curves in the lower two spectra are calculated spectra for symmetric interfaces. Note that the asymmetric interfaces give satellites that are less intense relative to the central peak than do the symmetric interfaces.

(d) *6-Å Cr series.* The selective orientation behavior (rule 2) as well as the effect of Cr being the layer that tends to strengthen the MLC growth can be seen strikingly in a series of ML's having ~ 6 Å of Cr and varying thicknesses of Co. The measured and calculated large-angle Cr $K\alpha$ x-ray spectra are shown in Fig. 7. The results of the linear-interface–model analysis are shown by the dotted curves and are summarized in Table VI. As discussed previously, the heights and positions of the satellites are dependent on the interface and bilayer thicknesses. In this case, since no satellites are seen, except slightly in the (14 Å)/(6 Å) ML, there is no sensitivity between the asymmetric and symmetric interface models. Thus the spectra were analyzed with only the symmetric model and only the total interface thicknesses are listed in Table VI. As seen in Fig. 7, the spectrum of the (6 Å)/(6 Å) ML is mainly a single interference peak between the positions of the [10.1] Co and [110] Cr as expected for an ML composed of alternating layers of these two orientations. There is also a small amount of type-*B* crystallites present in this ML. As the Co layer thickness increases the fraction of MLC's decreases drastically and the position of the MLC peak moves to higher angles in keeping with the larger Co content. For all spectra the highest-angle peak is due to MLC's and the other peaks are due to *B* and *C* crystallites. As seen in Table VI, the MLC lengths in the direction of growth decrease almost linearly with Λ from 140 to 55 Å, while the amount and lengths of the *B* and [10.0] Co crystallites strongly increase as Λ increases. As can be seen, by the low background, there are essentially no unaligned crystallites in this series. Thus a small amount of Cr is causing growth of MLC's, even for Co layers as thick as ~ 23 Å; however, $\sim 77\%$ of the (23 Å)/(6 Å) ML is made up of crystallites of pure Co.

4. SAXS spectra

The small-angle scattering spectra of several ML's were obtained using Cr $K\alpha$ x rays. Due to the similar atomic numbers of Co and Cr, this scattering is weak so that only 2–4 orders of scattering were seen. The bilayer thicknesses obtained from SAXS, after making corrections for refraction of the x rays and for offset from the focusing circle, were within 8% of those determined from LAXS.

B. Interface thicknesses from saturation magnetization

The large number of itinerant *d* electrons in Cr causes the first node of the Ruderman-Kittel-Kasuya-Yoshida

TABLE VI. Derived parameters for the nominal 6-Å Cr series. F and R are the front and rear surfaces.

Co/Cr (Å)	$(F+R)$,Cr,Co (no. of layers)	Λ (Å)	L_M (Å)	t_B,t_C	f_B,f_C	v_{ML},v_B,v_C (%)
6/6	4/1/1	12	138	51,0	0.16,0	94,6,0
14/6	4/1/5	20	102	81,54	0.54,0.02	69,30,1
17/6	6/0/6	23	64	183,109	1.00,0.01	25,74,1
23/6	6/0/9	29	55	193,174	0.92,0.60	23,72,5

polarization at Co atoms in the vicinity of Cr atoms to occur at smaller distances than in the pure Co. This results in the ferromagnetic alignment of Co being rapidly lost upon being alloyed with Cr and *Co*Cr alloys becoming nonmagnetic at 0 K at ~25 at. % Cr.[23] This behavior can be used to our advantage in analyzing the saturation-magnetization behavior of these ML's by assuming that the decrease in magnetization from that of bulk Co is due to Co atoms being in the interfaces. Under the assumptions discussed below, we can then estimate the thickness of the interfacial regions from the measured saturation-magnetization values M_{meas}. These values are taken as the magnetization measured in an applied field of 25 kOe at 4.5 K with a SHE-968 superconducting quantum-interference device (SQUID) magnetometer. Due to uncertainties in the area and thickness of the samples, we estimate that the M_{meas} values are known to only 10%.

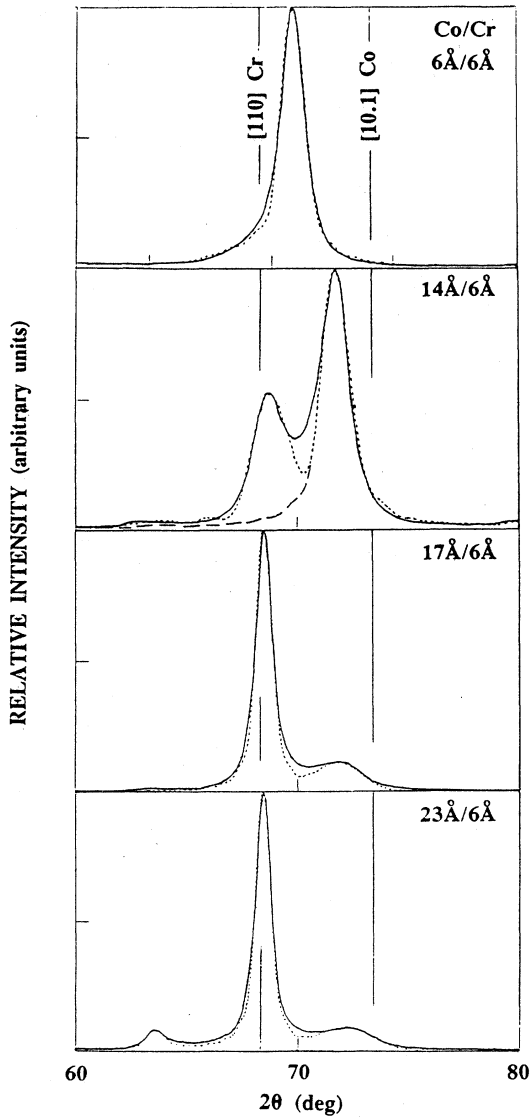

FIG. 7. Measured and calculated Cr $K\alpha$ x-ray spectra of a series of 6-Å Cr ML's. The solid and dotted curves are the measured and calculated spectra, respectively. The higher-angle peak is due to ML crystallites.

Using the linear-interface model described earlier and assuming that the magnetization decreases linearly from that in pure Co, M_{Co}, to zero at 25 at. % Cr for the Co atoms in the interfaces of the ML's, the saturation magnetization from the interfacial regions of the MLC's is given by

$$M_I \propto M_{\text{Co}} \int_0^{0.25} [1-t/(0.25t_I)](1-t/t_I)dt \ . \tag{3}$$

The factor $(1-t/t_I)$ is due to the variation of Co concentration and the other factor is due to the magnetization variation in the interfaces. The saturation magnetization of the MLC's, M_{ML}, is then given by

$$M_{\text{ML}} = (0.114t_I + t_{\text{Co}})M_{\text{Co}}/\Lambda \ , \tag{4}$$

where t_I is the total interface thickness and t_{Co} is the thickness of the pure-Co region. However, we have seen that in most Co/Cr ML's, that besides a fraction, f_{ML}, of the MLC's, there is a fraction, f_{bkg} (bkg denotes background), of the ML's which is unaligned in the direction of growth as well as fractions, f_{Co} and f_{Cr}, of aligned pure-Co and -Cr crystallites. Thus, in general, M_{meas} is made up of contributions from all these regions and is given by

$$M_{\text{meas}} = f_{\text{bkg}}M_{\text{bkg}} + f_{\text{Co}}M_{\text{Co}} + f_{\text{ML}}M_{\text{ML}} \ . \tag{5}$$

We want to obtain M_{ML} from M_{meas} and then use Eq. (4) to estimate t_I. For most Co/Cr ML's the quantities f_{bkg}, M_{bkg}, f_{Co}, and f_{ML} are unknown and thus M_{ML} cannot be obtained from M_{meas}. The conditions under which we can reliably estimate t_I from M_{meas} are when (1) there is negligible unaligned background in the x-ray spectra, $f_{\text{bkg}}=0$, and (2) there is a negligible amount of aligned pure crystallites, $f_{\text{Co}}=f_{\text{Cr}}=0$. Under these conditions $M_{\text{ML}}=M_{\text{meas}}$ and Eq. (4) can be used to obtain t_I. In this case we have

TABLE VII. Total interface thickness t_I derived from the saturation magnetization as described in the text. $M_{Co}=1475$ G.

Co/Cr (Å)	D_{Co} (Å)	Λ (Å)	M_{meas} (G)	Sat. magn.	t_I (Å) x ray A	S
6/6	6	12	404	8.5	8	8
6/8	6	14	113	12.5	8	12
12/14	12	26	294	17.5	20	25
21/14	21	35	691	13	16	24
22/22	22	44	468	20	22	28
22/19	22	41	522	20	22	30

$$t_I=2.594(D_{Co}-\Lambda M_{ML}/M_{Co}) , \quad (6)$$

where D_{Co} is the total thickness of Co in a bilayer, $D_{Co}=t_{Co}+t_I/2$. In Table VII we list the t_I values determined from the measured saturation magnetization values for those ML's which satisfy the above criteria. We also list the interface thicknesses obtained from fitting the x-ray spectra with the symmetric and asymmetric linear-interface models. We see that, except for the thinnest-layer samples, where the analysis is unreliable due to a lack of satellites, the t_I values obtained from the saturation-magnetization measurements are in fair agreement with the interface thicknesses from the x-ray analysis using asymmetric interfaces. The t_I values from the symmetric interface model tend to be too large; so again we have an indication that mainly the Co is diffusing or penetrating into the Cr during the deposition process.

V. DISCUSSION AND CONCLUSIONS

Since the Co/Cr multilayer system has poor lattice matching, ~3%, it is an ideal system in which to observe a variety of growth properties from LAXS spectra. The alignment in the direction of growth follows three empirical rules. The most novel one is that the growth orientations selected are those for which the area per atom is most closely matched. This alignment is sensitive to the deposition rates and substrate temperatures. The ML's are amorphous at low substrate temperatures and optimally aligned near room temperature with roughened growth at higher substrate temperatures.

The detailed structure of the multilayers was determined by fitting the calculated LAXS to the measured spectra. The main results of the analysis of several different series of ML's with equal and nonequal layer thickness are as follows.

(1) Due to the tendency of columnar growth in this system and the complex structure of the hcp lattice, the multilayers above certain layer thicknesses contain an appreciable fraction of oriented crystallites of pure Co and Cr.

(2) For equal-layer-thickness ML's the crystallites of multilayer material have a maximum length in the growth direction of ~200 Å at a bilayer thickness of ~30 Å, although the number of coherent bilayers decreases with increasing bilayer thickness over the whole series. The interface thickness increases as Λ increases to ~70 Å and then levels off at about a total interface thickness of ~30 Å. The order of the bilayers is very definite for MLC's with three or fewer bilayers.

(3) There is strong evidence from the 21-Å Co series that the interfaces are asymmetrical in a manner that indicates that Co mainly diffuses or penetrates into the Cr during deposition. The weakest link in ML crystallite growth is in the [10.1] Co layers.

(4) Some MLC's were always present in a ML series with a Cr thickness of only 6 Å, but the fraction decreases rapidly as the thickness of the Co layers increases.

HREM images of the ML's show strong columnar growth with the layered structure existing within the columns. As expected, the layers become rougher as their distance from the substrate increases. Thus the layers that are deposited later in the sequence are made up of quite jumbled ML crystallites. This behavior is clearly seen in the HREM images shown in Refs. 10, 14, and 24. Many more extensive studies with various electron-spectroscopy techniques have and are being performed on these ML's and these results are planned to be reported elsewhere.

ACKNOWLEDGMENTS

This work was partially supported by a National Science Foundation (NSF) Grant No. DMR-8610863.

*Present address: Department of Chemistry, Arizona State University, Tempe, AZ 85287.

[1]See, for example, D. B. McWhan, *Synthetic Modulated Structures,* edited by L. L. Chang and B. C. Giessen (Academic, New York, 1985).

[2]E. Bauer and J. H. van der Merwe, Phys. Rev. B **33**, 3657 (1986).

[3]S. A. Chambers, T. J. Wagener, and J. H. Weaver, Phys. Rev. B **36**, 8992 (1987).

[4]R. Kern, G. LeLay, and J. J. Metois, Curr. Top. Mater. Sci. **3**,

130 (1979).
[5]M. B. Stearns, Phys. Rev. B **38**, 8109 (1988).
[6]J. A. Venables, G. D. T. Spiller, and M. Hanbucken, Rep. Prog. Phys. **47**, 399 (1984).
[7]J. K. MacKenzie, A. J. W. Moore, and J. F. Nicholas, J. Phys. Chem. Solids, **23**, 185 (1962).
[8]F. J. A. den Broeder, D. Kuiper, A. P. van de Mosselaer, and W. Hoving, Phys. Rev. Lett. **60**, 2769 (1988).
[9]C. H. Lee, H. He, F. Lamelas, W. Vavra, C. Uher, and R. Clarke, Phys. Rev. Lett. **62**, 653 (1989).
[10]M. B. Stearns, C. H. Lee, C.-H. Chang, and A. K. Petford-Long, in *Metallic Multilayers and Epitaxy,* edited by M. Hong, S. Wolf, and D. C. Gubser (The Metallurgical Society of AIME, Denver, CO, 1988).
[11]A. Segmuller and A. E. Blakeslee, J. Appl. Crystallogr. **6**, 19 (1973).
[12]D. B. McWhan, M. Gurvitch, J. M. Rowell, and L. R. Walker, J. Appl. Phys. **54**, 3886 (1983).
[13]A. K. Petford-Long, M. B. Stearns, C.-H. Chang, S. R. Nutt, D. G. Stearns, N. M. Ceglio, and A. M. Hawryluk, J. Appl. Phys. **61**, 1422 (1987).
[14]S.-C. Y. Tsen, M. B. Stearns, and D. J. Smith (unpublished).
[15]Joint Committee on Powder Diffraction Standards Files, International Center for Diffraction Data, Swarthmore, PA 1988.
[16]T. Wielinga, J. C. Lodder, and J. Worst, IEEE Trans. Magn. **MAG-18**, 1107 (1982); Thin Solid Films **101**, 61 (1983).
[17]J. Q. Zheng, J. B. Ketterson, and G. P. Felcher, J. Appl. Phys. **53**, 3624 (1982).
[18]D. J. Webb, R. G. Walmsley, K. Parvin, P. H. Dickinson, T. H. Geballe, and R. M. White, Phys. Rev. B **32**, 4667 (1985).
[19]M. B. Stearns, C. H. Lee, and S. P. Vernon, J. Magn. Magn. Mater. **54-57**, 791 (1986).
[20]I. K. Schuller, Phys. Rev. Lett. **44**, 1597 (1980).
[21]A. Walmsley, J. Thompson, D. Friedman, R. W. White, and T. H. Geballe, IEEE Trans. Magn. **MAG-19**, 1992 (1983).
[22]H. Hahn and R. S. Averback, Phys. Rev. B **37**, 6533 (1988).
[23]R. M. Bozorth, *Ferromagnetism* (Van Nostrand, New York, 1951).
[24]A. K. Petford-Long, N. J. Long, and M. B. Stearns (unpublished).